

CrossMark  
click for updatesCite this: *RSC Adv.*, 2016, 6, 52695

# Low-density superhard materials: computational study of Li-inserted B-substituted closo-carboranes $\text{LiBC}_{11}$ and $\text{Li}_2\text{B}_2\text{C}_{10}$

Xiaolei Feng,<sup>a</sup> Xinyu Zhang,<sup>a</sup> Hanyu Liu,<sup>b</sup> Xin Qu,<sup>cd</sup> Simon A. T. Redfern,<sup>e</sup> John S. Tse<sup>\*ab</sup> and Quan Li<sup>\*a</sup>

Insertion of Li atoms into a B-substituted carbon cage produces two superhard compounds with relatively low density:  $\text{LiBC}_{11}$  and  $\text{Li}_2\text{B}_2\text{C}_{10}$ . For each structure, phonon frequencies across the whole Brillouin zone are positive, indicating dynamic stability. Electronic structure calculations indicate that they are semiconductors under ambient conditions. Estimates of the Vickers hardness, based on a semi-empirical model, highlight the incompressible nature of these two compounds. We then performed calculations on the ideal strengths of these two structures to confirm the hardness and investigate origins of the mechanical properties. Strikingly, both  $\text{LiBC}_{11}$  and  $\text{Li}_2\text{B}_2\text{C}_{10}$  can be classed as superhard materials, with hardness values of 49 GPa and 41 GPa, respectively. The current results shed light on the properties of new superhard carbon cage structures more generally.

Received 20th April 2016  
Accepted 23rd May 2016

DOI: 10.1039/c6ra10177a

www.rsc.org/advances

## Introduction

The search for superhard materials with Vickers hardness,  $H_v \geq 40$  GPa has been an important focus for some time in materials science and technology. A well-known family of superhard materials is that comprising light element compounds (such as  $\text{C}_3\text{N}$ ,<sup>1</sup>  $\text{B}_2\text{CO}$ ,<sup>2</sup>  $\text{BC}_2\text{N}$ ,<sup>3,4</sup>  $\text{B}_3\text{NO}$ ,<sup>5</sup> diamond,  $\text{BC}_3$ ,<sup>6,7</sup>  $\text{BC}_5$ ,<sup>8,9</sup>  $\text{BC}_7$ ,<sup>10</sup>  $\text{B}_6\text{O}$ ,<sup>11</sup> *pnnm*-CN,<sup>12</sup>  $\text{CN}_2$ ,<sup>13</sup>  $\text{BC}_2\text{N}$ ,<sup>14,15</sup> and *c*-BN<sup>16</sup>), where strong covalent bonding between light elements often leads to the formation of rigid three-dimensional crystalline networks with extreme resistance against stresses across a wide range of loading conditions. The low thermal stability of diamond in oxidizing environments and the high synthetic cost of these traditional superhard materials, have stimulated the search for novel superhard materials exhibiting improved stability over a wide range of conditions with good properties.

Sodalite-like cages (named after the cage zeolitic oxide) formed by groups of 12 atoms are thought to be the root of some extraordinary properties. A good example is a new clathrate sodalite-like structure of BN, which has recently been predicted to be “superhard”, with a hardness of 58.4 GPa.<sup>17</sup> Considering

the important role carbon plays in the materials world, it is interesting to explore the effects of inserting metal atoms into sodalite-like C cages. With larger atomic radii, C cages display relatively smaller cavities, even for the smallest metal atom (we consider Li atoms in this work). This inevitably leads to structural destabilization: here we seek to explain the electronic origins of such destabilization. Since a closed-shell electron configuration is helpful to stabilise a compound, and the C atoms forming the cages form already have a closed-shell electronic configuration, the insertion of electropositive Li atoms donate electrons to the antibonding bands and weaken the bonding. The insertion of Li does not, of itself, lead to superior hardness, but it does stabilise superhard phases. It is necessary to maintain the strong chemical bonds by adjusting the number of electrons in the system. One possible solution is to substitute C atoms with electron deficient B atoms in the framework as proposed by Tao Zeng *et al.* in their recent work.<sup>18</sup> In fact, isolated closo-carboranes, like 1,5- $\text{C}_2\text{B}_3\text{H}_5$ , 1,6- $\text{C}_2\text{B}_4\text{H}_6$ , 2,4- $\text{C}_2\text{B}_5\text{H}_7$ , have been synthesised experimentally,<sup>19</sup> therefore there is a good possibility that the bulk solid closo-carboranes may also be synthesised.

We explored the possibility of stabilizing the sodalite-like C cage by two strategies of coupled Li-insertion – B-substitution and proposed two compounds ( $\text{LiBC}_{11}$  and  $\text{Li}_2\text{B}_2\text{C}_{10}$ ), stable at ambient conditions. Electronic structure calculations suggest that both compounds are semiconductors with band gaps of 0.6–1.3 eV. Subsequent first-principles study of their mechanical properties indicates that both compounds are superhard. Moreover, they are also the lightest compounds among the family of known light element superhard materials. The predicted stable, superhard, Li/B/C ternary compounds, with

<sup>a</sup>State Key Laboratory of Superhard Materials and College of Materials Science and Engineering, Jilin University, Changchun, 130012, China. E-mail: liquan777@jlu.edu.cn

<sup>b</sup>Department of Physics and Engineering Physics, University of Saskatchewan, Saskatoon, Saskatchewan S7N 5E2, Canada. E-mail: john.tse@usask.ca

<sup>c</sup>Changchun Institute of Optics, Fine Mechanics and Physics, Chinese Academy of Sciences, Changchun 130033, P. R. China

<sup>d</sup>University of Chinese Academy of Sciences, Beijing 100039, P. R. China

<sup>e</sup>Department of Earth Sciences, University of Cambridge, Cambridge, CB2 3EQ, UK

remarkably low density, may have great potential importance for technological application and shed light on the general principles on the rational design of superhard structures.

## Computational methods

First-principles electronic structure calculations were based on density functional theory (DFT) and performed using the Vienna *ab initio* simulation package (VASP).<sup>20</sup> The generalised gradient approximation (GGA) in the scheme of Perdew–Burke–Ernzerh of (PBE)<sup>21</sup> was used to describe the electron exchange correlation interactions, while electron–ion interactions were treated using projected-augmented-wave (PAW) potentials.<sup>22</sup> PAW potentials with  $1s^2 2s^1$ ,  $2s^2 2p^1$ , and  $2s^2 2p^2$  electrons as valence electrons were adopted for the Li, B, and C atoms, respectively. A kinetic-energy cutoff of 720 eV and Monkhorst–Pack<sup>23</sup> meshes for Brillouin zone sampling with a resolution of  $0.01 \text{ \AA}^{-1}$  were chosen. The atomic relaxation was terminated when the change in the total energy per atom converged to less than 1 meV. To confirm the dynamical stability of the structures, we computed the phonon dispersions using a supercell approach as implemented in PHONOPY code<sup>24,25</sup> with  $2 \times 2 \times 2$  supercells. Elastic constants were computed from the strain–stress method, and the bulk and shear moduli were thus derived from the Voigt–Reuss–Hill averaging scheme.<sup>26</sup> The Vickers hardness was first estimated from a semi-empirical microscopic hardness model.<sup>27</sup> The exact stress–strain relation was then obtained explicitly by calculating the stress response to structural deformation along specific loading paths using a quasi-static relaxation method. The latter method can simulate various loading conditions and determine the corresponding ideal strength and deformation modes.<sup>28–31</sup>

## Results and discussion

The sodalite-like carbon cage adopts a remarkable cubic configuration ( $Im\bar{3}m$ , Pearson symbol cF14), with all 12 carbon atoms sharing identical point symmetry {Fig. 1(c)}. The calculated cubic cell parameter is in good agreement with the hypothetical structure proposed by Filipe *et al.*<sup>32</sup> The small difference (0.98%) between our calculated cubic unit cell lattice parameter and that of Filipe *et al.*<sup>32</sup> can be explained by the different electron exchange correlation interactions chosen (PBE in this work and LDA in ref. 32). To maintain the total number of electrons after inserting a Li atom into the cavity, we

replaced one of the framework C atoms with a B and then the structure was fully re-optimised. The resulting  $\text{LiBC}_{11}$  maintains the framework topology although the cage is slightly deformed. We further placed two Li atoms into two cavities formed by a double B-substituted C cage. In this case, there are five distinct ways for the double B substitutions. We examined all the possibilities and found that the most energetically favourable structure is to replace two non-adjacent atoms of one C–C bond. This configuration is in agreement with a previous study.<sup>18</sup> The unit cells of the resulting  $\text{LiBC}_{11}$  and  $\text{Li}_2\text{B}_2\text{C}_{10}$  (lowest enthalpy) structures are shown in Fig. 1, and the corresponding equilibrium structural parameters and space group at ambient pressure are listed in Table 1. The bond length of B–C is 1.63 Å and C–C bond lengths range from 1.55 Å to 1.60 Å in  $\text{LiBC}_{11}$ . In  $\text{Li}_2\text{B}_2\text{C}_{10}$ , the B–C bond length is 1.65 Å while C–C bond lengths are 1.57/1.59 Å.

To investigate the electron structure, the valence band structures and the corresponding density of states projected onto the atomic orbits (PDOS) were computed and the results are shown in Fig. 2. Here, the zero energy refers to the top of the valence band.  $\text{LiBC}_{11}$  and  $\text{Li}_2\text{B}_2\text{C}_{10}$  are both semiconductors characterised by indirect band gaps of 1.3 eV and 0.6 eV, respectively. The HSE hybrid functional usually provides a better description of the electronic band structure<sup>33,34</sup> (especially the band positions), but is computationally costly. In view of the fact that density functional theory, especially the semi-local PBE functional we used here, tends to underestimate the band gap of this class of compounds by 30–50%, we predict the experimental band gaps should be in the range of 1.9–2.6 eV and 0.9–1.2 eV for  $\text{LiBC}_{11}$  and  $\text{Li}_2\text{B}_2\text{C}_{10}$ , respectively. These values are considerably smaller than these of other light-element superhard materials (such as diamond,  $\text{BC}_3$ ,  $\text{BC}_5$ ,  $\text{BC}_2\text{N}$ , and cubic BN), which typically have band-gaps ranging from 3.0 eV to 3.6 eV. The small band gaps may suggest potential optical applications of these materials. A smaller gap is expected as an Li atom is introduced into the system since it will occupy the bottom of the conduction band. When a second B is inserted into the structure, the bottom of the conduction band [in Fig. 2(c)] is lowered, resulting an even lower band gap compared with that in Fig. 2(a), the PDOS plots demonstrate that C-2p electrons contribute most to both the upper conduction bands and lower valence bands.

The calculated electron localization functions show both  $\text{LiBC}_{11}$  and  $\text{Li}_2\text{B}_2\text{C}_{10}$  are ionic with the Li atoms donating their valence electrons to the B such that the effective configuration of B becomes  $s^2 p^2$ , as for the carbon. The ionic  $\text{LiBC}_{11}$  and  $\text{Li}_2\text{B}_2\text{C}_{10}$  compounds are isoelectronic with the  $\text{C}_{12}$  cage. Therefore, the strong covalent bonding between C–C and B–C are maintained thus preserving the stability of the rigid three-dimensional crystalline networks.

In Table 2, information on the calculated volume per unit cell, the volume per atom and the density of  $\text{LiBC}_{11}$  and  $\text{Li}_2\text{B}_2\text{C}_{10}$  are listed. Comparisons are made with the corresponding values for the empty  $\text{C}_{12}$  cage structure and for several previously proposed light-element superhard materials. It can be seen that the cage structures display larger volumes than non-cage structures. Specifically, the volume of the unit cell of

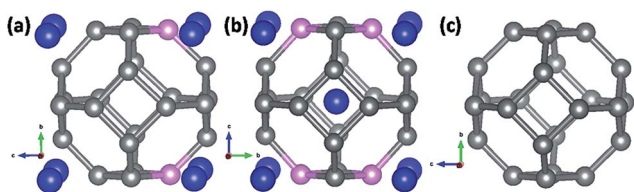
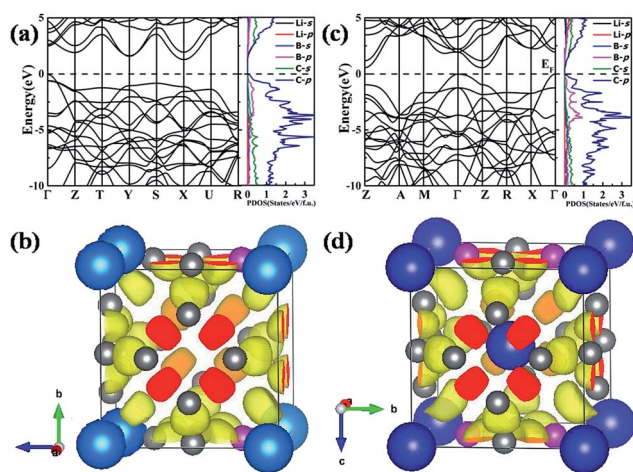


Fig. 1 Crystal structures of (a)  $\text{LiBC}_{11}$ , (b)  $\text{Li}_2\text{B}_2\text{C}_{10}$  and (c)  $\text{C}_{12}$ . The Li atoms are represented as large blue spheres, while B and C atoms are represented as small spheres, pink and grey respectively.

**Table 1** The space group and calculated equilibrium structural parameters: cubic unit cell parameters and Wychoff positions of LiBC<sub>11</sub> and Li<sub>2</sub>B<sub>2</sub>C<sub>10</sub> at ambient pressure

Phase	Space group	Lattice parameter (Å)	Atomic coordinates ( <i>r/a</i> , fractional)
C <sub>12</sub>	<i>Im</i> $\bar{3}m$	<i>a</i> = 4.383 <i>a</i> = 4.34 (ref. 32)	C 12d (0.000, 0.250, 0.500)
LiBC <sub>11</sub>	<i>Pmm</i> 2	<i>a</i> = 4.470  <i>b</i> = 4.469  <i>c</i> = 4.441	Li 1a (0.000, 0.000, 0.058) B 1c (0.500, 0.000, 0.249) C 2e (0.240, 0.000, 0.504) C 2g (0.000, 0.251, 0.504) C 2h (0.500, 0.257, 0.986) C 2f (0.250, 0.500, 0.988) C 1b (0.000, 0.500, 0.244) C 1b (0.000, 0.500, 0.745) C 1c (0.500, 0.000, 0.743)
Li <sub>2</sub> B <sub>2</sub> C <sub>10</sub>	<i>P4</i> <sub>2</sub> / <i>mnm</i>	<i>a</i> = 4.578 <i>c</i> = 4.424	Li 2d (0.250, 0.000, 0.000) B 2e (0.000, 0.000, 0.250) C 4m (0.500, 0.749, 0.500) C 2f (0.500, 0.500, 0.250) C 4j (0.734, 0.000, 0.000)

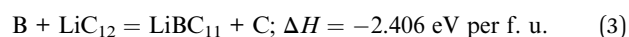
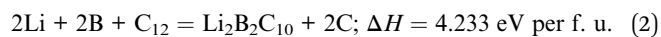
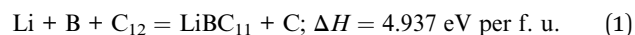
**Fig. 2** Calculated band structures and PDOS for (a) LiBC<sub>11</sub> and (c) Li<sub>2</sub>B<sub>2</sub>C<sub>10</sub>; calculated electron localization function (isosurfaces = 0.8) for (b) LiBC<sub>11</sub> and (d) Li<sub>2</sub>B<sub>2</sub>C<sub>10</sub>, at 0 GPa.**Table 2** The calculated volume per unit cell, the volume per atom and density for LiBC<sub>11</sub>, Li<sub>2</sub>B<sub>2</sub>C<sub>10</sub> and earlier proposed light elements superhard materials

Structure	Volume (Å <sup>3</sup> per unit cell)	Volume (Å <sup>3</sup> per atom)	Density (g cm <sup>-3</sup> )
C <sub>12</sub>	81.75	6.81	2.843
C <sub>12</sub> (ref. 32)	82.08	6.84	2.928
LiBC <sub>11</sub>	88.71	6.82	2.805
Li <sub>2</sub> B <sub>2</sub> C <sub>10</sub>	92.71	6.62	2.787
Diamond	11.35	5.68	3.510
c-BN	11.83	5.92	3.483
BC <sub>5</sub>	36.02	6.00	3.265

Li<sub>2</sub>B<sub>2</sub>C<sub>10</sub> (92.71 Å<sup>3</sup>) is substantially larger than that of LiBC<sub>11</sub> (88.71 Å<sup>3</sup>). The volume per atom (the volume per unit cell divided by the total number of atoms in the unit cell) shows the

same trend as the volume per unit cell: 6.82 Å<sup>3</sup> per atom and 6.60 Å<sup>3</sup> per atom for caged LiBC<sub>11</sub> and Li<sub>2</sub>B<sub>2</sub>C<sub>10</sub>, respectively, in contrast to smaller values (ranging from 5.68 to 6.00 Å<sup>3</sup> per atom) for other materials. The densities for LiBC<sub>11</sub> and Li<sub>2</sub>B<sub>2</sub>C<sub>10</sub> are 2.805 and 2.787 g cm<sup>-3</sup>, respectively. These values are much lower than the densities of other well-known superhard materials such as 3.510 g cm<sup>-3</sup> for diamond, 3.483 g cm<sup>-3</sup> for c-BN and 3.265 g cm<sup>-3</sup> for BC<sub>5</sub>. It is worth noting that even though Li<sub>2</sub>B<sub>2</sub>C<sub>10</sub> has a smaller volume per atom than LiBC<sub>11</sub>, because the formula unit contains more light atoms, it is less dense than LiBC<sub>11</sub>, making it the lightest superhard material reported. This property may be related to the unexpected and so-far unidentified hard and transparent carbon phase found in a rock sample with an estimated density of 2.5 g cm<sup>-3</sup> from the Popigai impact crater in Russia.<sup>35</sup>

The thermodynamic stability of the two Li-B-carbides with respect to the decomposition into the respective elements, can be quantified by the formation enthalpies of two different reaction routes. The positive reaction enthalpies of reactions (1) and (2) below indicate that LiBC<sub>11</sub> and Li<sub>2</sub>B<sub>2</sub>C<sub>10</sub> are thermodynamically metastable. Li-substitution, as expected, is highly endothermic, as seen in reactions (3) and (4). B-Substitution helps to stabilise Li-insertion into the carbon cages. The successful synthesis of several isolated closo-carboranes, like 1,5-C<sub>2</sub>B<sub>3</sub>H<sub>5</sub>, 1,6-C<sub>2</sub>B<sub>4</sub>H<sub>6</sub>, 2,4-C<sub>2</sub>B<sub>5</sub>H<sub>7</sub>,<sup>19</sup> indicate that there is a good possibility that the bulk solid closo-carboranes can be also synthesised although there are experimental challenges to overcome the activation barriers. Nonetheless, the example of the existence of metastable diamond demonstrates that routes to the synthesis of these compounds may indeed be tractable.



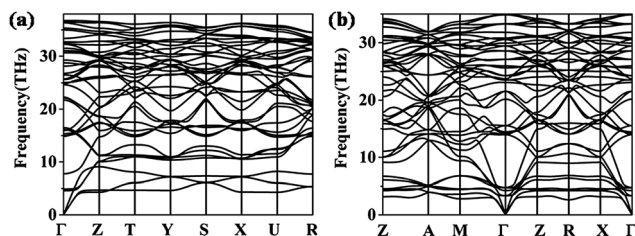
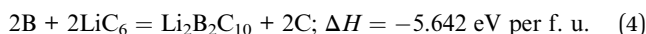


Fig. 3 Calculated phonon dispersion curves for (a) LiBC<sub>11</sub> and (b) Li<sub>2</sub>B<sub>2</sub>C<sub>10</sub>, at 0 GPa.



The structural stability of both LiBC<sub>11</sub> and Li<sub>2</sub>B<sub>2</sub>C<sub>10</sub> has been investigated by calculations of their phonon band structures and elastic constants. As can be seen in Fig. 3, there are no imaginary phonons in the Brillouin zone for both LiBC<sub>11</sub> and Li<sub>2</sub>B<sub>2</sub>C<sub>10</sub>, confirming their dynamical stability. Based on the mechanical stability criteria<sup>36</sup> of orthorhombic or tetragonal crystals (where combinations of elastic constants have to exceed or equal zero), the calculated elastic constants also indicate that both LiBC<sub>11</sub> and Li<sub>2</sub>B<sub>2</sub>C<sub>10</sub> are mechanically stable under ambient pressure.

The mechanical hardness of a material is the ability to resist plastic deformation from hydrostatic compression, tensile load, and shear. Therefore, a superhard material usually requires a high bulk modulus ( $B_0$ ) to resist volume decrease created by compression and also high shear modulus ( $G_0$ ) to limit the creation and mobility of dislocations. In Table 3 we list the bulk and shear moduli of LiBC<sub>11</sub> and Li<sub>2</sub>B<sub>2</sub>C<sub>10</sub> derived from the calculated elastic constants. The calculated values for  $B_0$  of LiBC<sub>11</sub> and Li<sub>2</sub>B<sub>2</sub>C<sub>10</sub> are 302 GPa and 208 GPa, and  $G_0$  are calculated to be 271 GPa and 232 GPa, respectively, indicating the highly incompressible nature of these structures. We further estimated the Vickers hardness ( $H_v$ ) using an empirical model<sup>27</sup> based on the correlation of the shear modulus with hardness. A comparison with the empty C<sub>12</sub> cage structure is listed in Table 3. High hardness values of 48.8 GPa and 37.7 GPa are estimated for LiBC<sub>11</sub> and Li<sub>2</sub>B<sub>2</sub>C<sub>10</sub>, respectively. These values are slightly lower than that of the bare C<sub>12</sub> cage (51.5 GPa). To elucidate the microscopic mechanism of bond-deformation and breaking, we present below a first-principle strain–stress calculation, to further probe the mechanical properties of LiBC<sub>11</sub> and Li<sub>2</sub>B<sub>2</sub>C<sub>10</sub> under large structural deformations.

The ideal strength, the maximum stress that a material can sustain, is the upper bound to the critical stress for crack formation and dislocation nucleation in the material. When the applied stress exceeds the ideal strength, the crystal structure will collapse even at zero temperature. Therefore, a strain–stress

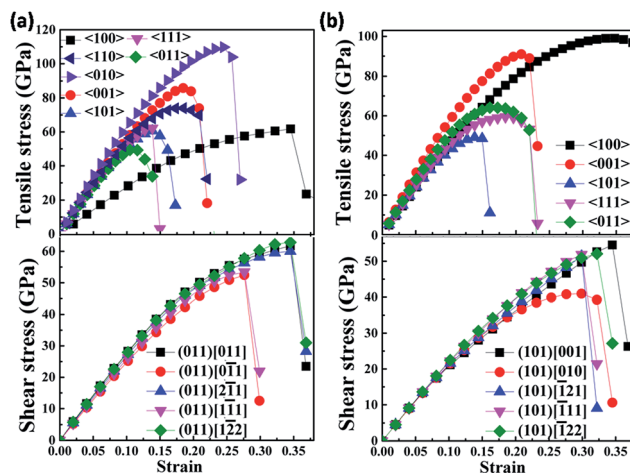


Fig. 4 The calculated strain–stress relation in various tensile (upper panels) and shear (lower panels) directions of (a) LiBC<sub>11</sub> and (b) Li<sub>2</sub>B<sub>2</sub>C<sub>10</sub> at 0 GPa, respectively.

calculation also serves to describe the upper bound limit of the hardness of a material.

We have examined the stress–strain relations of LiBC<sub>11</sub> and Li<sub>2</sub>B<sub>2</sub>C<sub>10</sub> under tensile loadings. The results are shown in Fig. 4 (upper panels). LiBC<sub>11</sub> shows remarkably strong stress response in the  $\langle 010 \rangle$  directions with the peak tensile stress reaching 110 GPa. The peak tensile stresses along the  $\langle 001 \rangle$ ,  $\langle 110 \rangle$ ,  $\langle 100 \rangle$ ,  $\langle 111 \rangle$ , and  $\langle 101 \rangle$  directions are also high, ranging from 62 GPa to 86 GPa. The lowest tensile strength, corresponding to the weakest direction, lies along the  $\langle 011 \rangle$  direction and peaks at 49 GPa. Our results show that when the tensile stress exceeds 49 GPa, the  $\{011\}$  type planes of the crystal first become unstable against cleavage fracture. For Li<sub>2</sub>B<sub>2</sub>C<sub>10</sub>, the highest tensile strength is 99 GPa along the  $\langle 100 \rangle$  directions, followed by 91 GPa along the  $\langle 001 \rangle$  directions. The weakest tensile strength is along  $\langle 101 \rangle$  type directions with a value of 49 GPa, indicating that Li<sub>2</sub>B<sub>2</sub>C<sub>10</sub> would fail by cleavage in the  $\langle 101 \rangle$  direction at 49 GPa. Similar to the estimations from the empirical model, the conclusion that LiBC<sub>11</sub> and Li<sub>2</sub>B<sub>2</sub>C<sub>10</sub> are both superhard is valid.

We now turn to ideal shear strength in the tensile-weakest (easiest-cleavage) plane. Various non-equivalent directions along the shear-sliding planes have been systematically studied under shear deformations, as shown in Fig. 4 (lower panels). It can be seen that the shear strengths of LiBC<sub>11</sub> range from 52 GPa to 63 GPa, with the weakest one being the  $\langle 011 \rangle[011]$  shear system with the value of 49 GPa. Therefore, the resulting hardness of LiBC<sub>11</sub> compound is calculated to be 49 GPa, which is in good agreement with the estimated value from the empirical microscopic hardness model (0.41%). For Li<sub>2</sub>B<sub>2</sub>C<sub>10</sub>,

Table 3 The calculated elastic constants  $C_{ij}$  (GPa), bulk modulus  $B_0$  (GPa), shear modulus  $G_0$  (GPa),  $G_0/B_0$  and Vickers hardness  $H_v$  of C<sub>12</sub>, LiBC<sub>11</sub> and Li<sub>2</sub>B<sub>2</sub>C<sub>10</sub>

Structure	$C_{11}$	$C_{22}$	$C_{33}$	$C_{44}$	$C_{55}$	$C_{66}$	$C_{12}$	$C_{13}$	$C_{23}$	$B_0$	$G_0$	$G_0/B_0$	$H_v$
C <sub>12</sub>	797			300			102			334	319	0.955	51.5
LiBC <sub>11</sub>	727	732	631	253	246	268	94	115	106	302	271	0.895	48.8
Li <sub>2</sub> B <sub>2</sub> C <sub>10</sub>	676		676	209		209	156	87		282	232	0.824	37.7

the shear strengths fall over a narrow range from 53 GPa to 56 GPa for most of the shear directions, apart from (101)[010] direction, along which the  $\text{Li}_2\text{B}_2\text{C}_{10}$  crystal is unstable against slip on crystallographic planes when the shear stress exceeds 41 GPa. The lowest shear strength of 41 GPa is smaller than the ideal tensile strength, suggesting that the hardness of  $\text{Li}_2\text{B}_2\text{C}_{10}$  is slightly lowered. Nevertheless, since the lowest shear strength surpasses the threshold (40 GPa), it still can be classified as superhard materials.

## Conclusion

Using first-principle calculations, we have investigated the structural, electronic, dynamical, and mechanical properties of two Li-doped B-substituted carbon cages:  $\text{LiBC}_{11}$  and  $\text{Li}_2\text{B}_2\text{C}_{10}$ . The electronic structures suggest that both compounds are semiconductors. Phonon dispersion and elastic constant calculations demonstrate that both are dynamically and mechanically stable at ambient condition. First-principles strain–stress relations at large strains were also computed to examine the structural and mechanical properties. The established ideal tensile strength of 49 GPa in the (011) direction and ideal shear strength of 41 GPa along (101)[010] direction both suggest that  $\text{LiBC}_{11}$  and  $\text{Li}_2\text{B}_2\text{C}_{10}$  may be regarded as superhard materials.

## Acknowledgements

X. F. and Q. L. acknowledge the funding supports from the National Natural Science Foundation of China under Grant No. 11474125, 11274136 and 11534003. J. T. and H. L. acknowledge the National Science Foundation of China (11474126) and support from the University of Saskatchewan research computing group and the use of the HPC resources (Plato machine).

## References

- 1 J. Hao, H. Liu, W. Lei, X. Tang, J. Lu, D. Liu and Y. Li, *J. Phys. Chem. C*, 2015, **119**(51), 28614–28619.
- 2 L. Yinwei, L. Quan and M. Yanming, *EPL*, 2011, **95**(6), 66006.
- 3 Q. Li, M. Wang, A. R. Oganov, T. Cui, Y. Ma and G. Zou, *J. Appl. Phys.*, 2009, **105**(5), 053514.
- 4 V. L. Solozhenko, D. Andrault, G. Fiquet, M. Mezouar and D. C. Rubie, *Appl. Phys. Lett.*, 2001, **78**(10), 1385.
- 5 Q. Li, J. Wang, M. Zhang, Q. Li and Y. Ma, *RSC Adv.*, 2015, **5**(45), 35882–35887.
- 6 H. Liu, Q. Li, L. Zhu and Y. Ma, *Phys. Lett. A*, 2011, **375**(3), 771–774.
- 7 M. Zhang, H. Liu, Q. Li, B. Gao, Y. Wang, H. Li, C. Chen and Y. Ma, *Phys. Rev. Lett.*, 2015, **114**(1), 015502.
- 8 L. Quan, W. Hui, T. Yongjun, X. Yang, C. Tian, H. Julong, M. Yanming and Z. Guangtian, *J. Appl. Phys.*, 2010, **108**(2), 023507.
- 9 V. L. Solozhenko, O. O. Kurakevych, D. Andrault, Y. Le Godec and M. Mezouar, *Phys. Rev. Lett.*, 2009, **102**(1), 015506.
- 10 H. Liu, Q. Li, L. Zhu and Y. Ma, *Solid State Commun.*, 2011, **151**(9), 716–719.
- 11 M. Kobayashi, I. Higashi, C. Brodhag and F. Thevenot, *J. Mater. Sci.*, 1993, **28**(8), 2129–2134.
- 12 X. Tang, J. Hao and Y. Li, *Phys. Chem. Chem. Phys.*, 2015, **17**(41), 27821–27825.
- 13 Q. Li, H. Liu, D. Zhou, W. Zheng, Z. Wu and Y. Ma, *Phys. Chem. Chem. Phys.*, 2012, **14**(37), 13081–13087.
- 14 Q. Li, M. Wang, A. R. Oganov, T. Cui, Y. Ma and G. Zou, *J. Appl. Phys.*, 2009, **105**(5), 53514.
- 15 Y. Zhang, H. Sun and C. Chen, *Phys. Rev. Lett.*, 2004, **93**(19), 195504.
- 16 R. Wentorf Jr, *J. Chem. Phys.*, 1957, **26**(4), 956.
- 17 Y. Li, J. Hao, H. Liu, S. Lu and J. S. Tse, *Phys. Rev. Lett.*, 2015, **115**(10), 105502.
- 18 T. Zeng, R. Hoffmann, R. Nesper, N. W. Ashcroft, T. A. Strobel and D. M. Proserpio, *J. Am. Chem. Soc.*, 2015, **137**(39), 12639–12652.
- 19 J. F. Ditter, E. B. Klusmann, J. D. Oakes and R. E. Williams, *Inorg. Chem.*, 1970, **9**(4), 889–892.
- 20 G. Kresse and J. Furthmüller, *Phys. Rev. B: Condens. Matter Mater. Phys.*, 1996, **54**(16), 11169–11186.
- 21 J. P. Perdew, K. Burke and M. Ernzerhof, *Phys. Rev. Lett.*, 1996, **77**(18), 3865–3868.
- 22 G. Kresse and D. Joubert, *Phys. Rev. B: Condens. Matter Mater. Phys.*, 1999, **59**(3), 1758–1775.
- 23 H. J. Monkhorst and J. D. Pack, *Phys. Rev. B: Solid State*, 1976, **13**(12), 5188–5192.
- 24 A. Togo and I. Tanaka, *Scr. Mater.*, 2015, **108**, 1–5.
- 25 A. Togo, F. Oba and I. Tanaka, *Phys. Rev. B: Condens. Matter Mater. Phys.*, 2008, **78**(13), 134106.
- 26 R. Hill, *Proc. Phys. Soc., London, Sect. A*, 1952, **65**(5), 349.
- 27 J. Tse, *J. Superhard Mater.*, 2010, **32**(3), 177–191.
- 28 M. Zhang, M. Lu, Y. Du, L. Gao, C. Lu and H. Liu, *J. Chem. Phys.*, 2014, **140**(17), 174505.
- 29 Z. Pan, H. Sun, Y. Zhang and C. Chen, *Phys. Rev. Lett.*, 2009, **102**(5), 055503.
- 30 K.-W. Sun, Y.-Y. Zhang and Q.-H. Chen, *Phys. Rev. B: Condens. Matter Mater. Phys.*, 2009, **79**(10), 104429.
- 31 Y. Zhang, H. Sun and C. Chen, *Phys. Rev. Lett.*, 2004, **93**(19), 195504.
- 32 F. J. Ribeiro, P. Tangney, S. G. Louie and M. L. Cohen, *Phys. Rev. B: Condens. Matter Mater. Phys.*, 2006, **74**(17), 172101.
- 33 B. Wong and J. Cordaro, *J. Phys. Chem. C*, 2011, **115**(37), 18333–18341.
- 34 B. Janesko, *J. Chem. Phys.*, 2011, **134**, 184105.
- 35 A. El Goresy, L. S. Dubrovinsky, P. Gillet, S. Mostefaoui, G. Graup, M. Drakopoulos, A. S. Simionovici, V. Swamy and V. L. Masaitis, *C. R. Geosci.*, 2003, **335**(12), 889–898.
- 36 J. F. Nye, *Physical properties of crystals: their representation by tensors and matrices*, Oxford University Press, 1985.